Journal of Chromatography B, 906 (2012) 33–40

Contents lists available at SciVerse ScienceDirect

Journal of Chromatography B

journal homepage: www.elsevier.com/locate/chromb

Identification of the urinary metabolites of glionitrin A in rats using ultra-performance liquid chromatography combined with quadrupole time-of-flight mass spectrometry

Soo Hyun Lee[a], Hyun Ok Yang[c], Hak Cheol Kwon[c], Byung Hwa Jung[a,b,*]

[a] Molecular Recognition Research Center, Korea Institute of Science and Technology, Seoul, Republic of Korea
[b] University of Science and Technology, 113 Gwahangno, Yuseong-gu, Daejeon 305-333, Republic of Korea
[c] Natural Medicine Center, Korea Institute of Science and Technology, Gangneung, Republic of Korea

ARTICLE INFO

Article history:
Received 14 March 2012
Accepted 12 August 2012
Available online 21 August 2012

Keywords:
Gliotrin A
Urinary metabolites
UPLC–QTOP-MS
Diketopiperazine disulfide

ABSTRACT

Glionitrin A (GN A) is a new diketopiperazine disulfide with an aromatic nitro group, which is isolated from the coculture of an *Aspergillus fumigatus* fungal strain and a Sphingomonas bacterial strain. After intravenous administration of GN A in rats, 13 urinary metabolites of GN A were identified using ultra-performance liquid chromatography/quadrupole time-of-flight mass spectroscopy (UPLC–QTOP-MS) analysis in conjunction with data processing programs such as MetaboLynx™ and MassFragnent™. Reduction, nitro-reduction and hydration were the primary metabolic processes affecting GN A *in vivo*, followed by demethylation or oxidative deamination to alcohol, as well as cysteine, glycine, glucuronide or sulfate conjugation. The metabolite resulting from reduction was found to be a molecule with a dithiol group, and the metabolite made by nitro reduction was found to be an aromatic amine corresponding to GN A. Both of these products may have pharmacological or toxicological activity, which is valuable information in terms of using GN A as a lead compound. In addition, this work showed that UPLC–QTOP-MS analysis coupled with efficient data processing programs is useful for rapid and reliable characterization of GN A metabolites *in vivo*.

1. Introduction

Glionitrin A (GN A) (Fig. 1) is a new diketopiperazine disulfide isolated from the coculture of the *Aspergillus fumigatus* fungal strain KMC-901 and the Sphingomonas bacterial strain KMK-001 [1]. Its structure is similar to gliotoxin and dehydrogliotoxin, but it is unique in that it has a nitro aromatic ring. It showed promising antimicrobial activities against several microbes, including methicillin-resistant *Staphylococcus aureus*. It also displayed significant cytotoxic capacities toward some human cancer cell lines in an *in vitro* MTT cytotoxicity assay [1]. These features suggest that glionitrin A might be a potential drug candidate.

The identification of the metabolites of potential drug candidates provides essential information on drug efficacy and the toxicological profile and also provides information that may result in the generation of new, improved drug structures. Lately, metabolic studies performed in the early stage of drug discovery have been applied to judge whether new molecules are worth further development [2]. Liquid chromatography/mass spectrometry (LC/MS) is highly useful for this application. In particular, the use of a high-resolution MS system with excellent accuracy and stability coupled with a sophisticated data processing program has guaranteed the quality and productivity of metabolite acquisition processes [3]. Additionally, ultra-performance liquid chromatography (UPLC) provides improvement in separation and resolution in a shorter time compared with conventional high-performance liquid chromatography (HPLC) [4].

In the present study, the potential metabolites of GN A *in vivo* were determined through an analytical process based on UPLC–QTOF-MS, followed by a data search with a well-designed, automated data analysis program. This approach efficiently provided high-quality structural information on GN A metabolites excreted in the urine after intravenous administration, even though the biotransformed molecules occurred at trace levels concomitant with an excess of endogenous compounds.

2. Materials and methods

2.1. Chemicals and reagents

GN A was isolated from the coculture of an *Aspergillus fumigatus* fungal strain and a Sphingomonas bacterial strain. The crude

* Corresponding author at: Biomolecules Function Research Center, Korea Institute of Science and Technology, P.O. Box 131, Cheongryang, Seoul 130-650, Republic of Korea. Tel.: +82 2 958 5062; fax: +82 2 958 5059.
E-mail address: jbhluck@kist.re.kr (B.H. Jung).

1570-0232/$ – see front matter © 2012 Elsevier B.V. All rights reserved.
http://dx.doi.org/10.1016/j.jchromb.2012.08.015

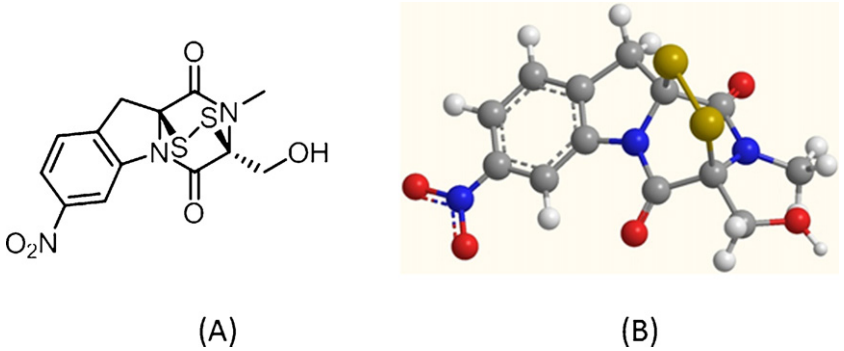

Fig. 1. Structure of GN A: (A) 2D structure and (B) 3D structure.

extract was fractionated by reverse-phase HPLC using gradient elution, and then GN A was purified by normal-phase HPLC followed by crystallization, which was precisely described in the previous report [1]. GN A crystals was dissolved in methanol at a concentration of 1 μg/ml and its purity was checked on chromatogram by UPLC–QTOF-MS analysis. Gliotoxin and acetonitrile (HPLC grade) and formic acid were purchased from Sigma-Aldrich Chemical Co. (St. Louis, MO, USA). Saline solution was purchase form Dai Han Pharm (Seoul, Korea). Ultrapure water (18.2 MΩ) was obtained using a Milli-Q apparatus from Millipore (Milford, USA).

2.2. Stability of GN A in saline and urine

Stabilities of GN A in saline and urine were tested according to the methods precisely explained in supplement materials. Here is brief description as follows: For urine stability test, 100 μl of quality control (QC) samples were prepared at lower (0.01 μg/ml), low (0.1 μg/ml), medium (1 μg/ml) and high (10 μg/ml) of GN A by spiking an appropriate amount in urine. Five replicates of each QC samples were evaluated in every condition of stability tests. To test short-term stability, QC samples were stored at room temperature for 0, 1, 2, 4 and 8 h as well as at 4 °C for 24 h. To evaluate the long-term stability, QC samples were stored at −80 °C for 2 and 4 weeks. The stability of GN A through the freeze (−80 °C) – thaw (room temperature) cycles were tested with QC samples that underwent the freeze and thawing process three times. For evaluation of stability in IV dosing solution, 100 μl of test sample was prepared at the concentration of 1 μg/ml of GN A by adding in saline. Five replicates were stored at room temperature for 0, 15, 30, 60 and 120 min. Each stability test was stopped by adding 200 μl of methanol containing gliotoxin (250 ng/ml; internal standard). Test samples were analyzed using LC–MS/MS and the percentages of GN A remaining at each time point relative to sample at the starting point were calculated. A compound was considered stable if the percentages at each time point were within ±15% of the sample at starting point.

2.3. Animal experiments

Eight-week-old male Sprague–Dawley rats (weighing 270–300 g) were purchased from Orientbio Korea (Seoul, Republic of Korea). The rats were housed in a room with an ambient temperature of 23 ± 2 °C, 12-h light/dark cycles, and a relative humidity of 55 ± 10% for 7 days. Rats were fasted for 12 h before drug injection and for a further 4 h after dosing. Water was available *ad libitum* during the experiments. For the drug injection, the jugular vein of each rat was cannulated using polyethylene tubing (PE50) under anesthesia with a 2:1 mixture of Zoletil® and Rompun®. Rats were administered a single intravenous (IV) dose of GN A dissolved in saline (10 mg/kg). Blank urine samples were collected before drug administration over 8 h and urine samples were collected for 8 h after IV injection. All urine samples were stored at −80 °C until analyzed. The animal experimental protocol was approved by the institutional animal care and use committee of Korea Institute of Science and Technology.

2.4. Sample preparation

A 200 μL aliquot of each urine sample was centrifuged at 10,000 × *g* for 15 min at 4 °C to remove particulates and was then diluted with the same volume of water. 200 μL of diluted urine was transferred to an autosampler vial. Five microliters of the prepared urine sample were injected into the UPLC-QTOF-MS system for analysis.

2.5. UPLC/ESI-QTOF-MS analysis

UPLC–QTOF-MS was used to identify GN A metabolites in rat urine. An ACQUIRY UPLC® (Waters, Milford, MA, USA) was directly connected to a QTOF-MS (SYNAPT™ G2, Waters, Milford, MA, USA). Separation was achieved using an Acquity UPLC BEH C18 column (1.7 μm particle size, 2.1 mm inner diameter, 100 mm length; Waters) at 40 °C. The gradient elution was performed using a mixture of solvent A (0.1% formic acid in 1% acetonitrile) and solvent B (0.1% formic acid in 99% acetonitrile) at a flow rate of 0.4 ml/min. The starting conditions were 100% A for 1 min, changing to 0% A at 17 min, and the solvent composition was then held at 100% B for 1 min. Re-equilibration of the system with 100% A (v/v) for 2 min was conducted prior to the next injection. All samples were kept at 4 °C during the analysis.

Mass spectrometry was performed in negative ionization mode with an electrospray ionization source (ESI) interface. The capillary voltage was set to 2500 V, and the cone voltage was 40 V. Nitrogen was used as the desolvation and cone gas at a flow rate of 600 L/h and 60 L/h, respectively. The source temperature was 120 °C, and the dissolution temperature was 350 °C. Leucine-enkephalin (0.2 μg/L in 50% methanol) was utilized as the lock mass (mass-to-charge ratio (*m*/*z*) 554.2615) at a flow rate 20 μL/min. Full scan data were collected at a range of *m*/*z* 50–1200 over a period of 15 min with a scan time of 0.5 s and an interscan delay of the 0.1 s. *m*/*z* values in resolution mode, and all of the acquired spectra were automatically corrected during acquisition based on the lock mass. The mass spectrometric data were collected into two separate data channels, using collision energy alternating between 0 (low-energy scans) and 30 eV (high-energy scans) in the centroid mode. Before analysis, the mass spectrometer was calibrated with 0.2 mM sodium formate solution.

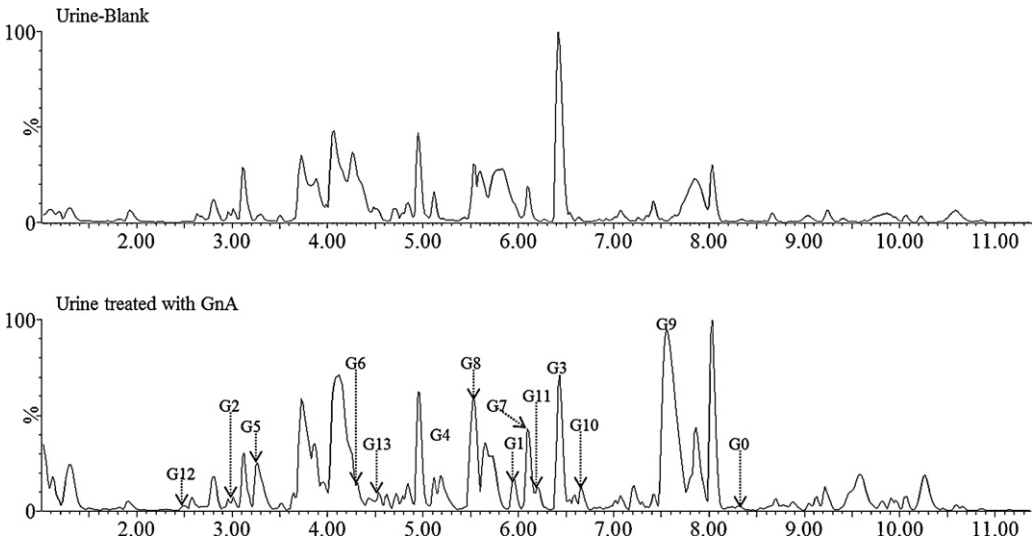

Fig. 2. Typical base peak intensity (BPI) chromatograms obtained from blank and drug-treated rat urine.

2.6. Data analysis

The raw mass spectrometry data from all of the samples were processed by a MetaboLynx XS version 4.1 (Waters Corp., Milford, USA), which employs a comprehensive list of potential biotransformation reactions with the elemental compositions of each possible metabolite and generates a sequence of extraction ion chromatograms (XICs). Comparing the XICs of the samples after GN A administration and blank samples allows for the identification of potential drug metabolites. The key analysis parameters were as follows. The tolerance of the mass defect filter (MDF) was set at 15 mDa. In the MS trace condition, the retention time ranged from 1 to 12 min. For expected MS chromatograms, mass values were estimated from the parent molecule (glionitrin A) and expected metabolites; unexpected metabolite chromatograms were presented from mass range chromatograms by a full acquisition mass ranging from 50 to 1000 Da. For integrated chromatogram conditions of expected and unexpected metabolites, the mass window was set at 0.05 Da and the response threshold was adapted at 10% of absolute area. In the spectrum condition, the intensity threshold of metabolite identification was 10%. In false positive conditions, the retention time window was set to a 0.1 min matching with a blank sample, the ratio of analyte to control peak area was 5, and false positive results were not reported. Elemental compositions for expected and unexpected metabolite peaks were created using an exhaustive list of potential formulas of the metabolites.

The structural prediction was performed using MassFragment™ software, which applied systematic bond disconnections and a specific scoring system to automatically present structural assignment in response to high mass accuracy and precision. The key parameters for the mass fragment analysis were as follows: maximum mass errors, less than 5 ppm; double-bond equivalent (DBE), 0–50; maximum H deficit, 6; electron count, both; and fragment number of bonds, 4.

3. Results and discussion

3.1. Chemical stability of GN A

To exclude the possibility that the observed putative metabolites of GN A are derived due to chemical instability of molecule, stability of GN A in urine and saline as well as its purity were tested. When the purity of GN A crystals was checked by UPLC–QTOF-MS analysis, its purity was estimated over 98% (Supple Fig. 1). As GN A was mainly stored as crystals and dissolved in saline right before injection, high purity of its crystal can guarantee its stability at storage condition and quality of injection material. To confirm its stability during the experiments, the change of GN A in urine and saline (used for IV injection) were checked. No significant change of GN A was observed at every condition of the stability test, implying that GN A was chemically stable during the experiments (Supple Tables 1 and 2). These results suggest that the potential metabolites of GN A presented in this study exclusively resulted from metabolism *in vivo*.

3.2. Metabolic profile of GN A

The UPLC–MS conditions were optimized to provide a full overview of the pattern of the metabolites in rat urine after administration of GN A. The acetonitrile–water system had better separation capacity and elution power than the methanol–water system. Ionization of parent GN A was much better in the negative ionization mode than in the positive mode, and the difference in the chromatograms of blank and drug-treated urine was more noticeable in the negative mode. Therefore, all processing for metabolite identification was performed in the negative ionization mode. MS data were acquired in the MS^E mode, which is a fast scanning method to obtain full-scan MS and MS–MS data simultaneously in a single run via collision energy switching. Typical base peak intensity (BPI) chromatograms from drug-treated and blank samples are shown in Fig. 2. When compared with blank samples, the parent compound and 13 metabolites were detected in rat urine in the negative ionization mode.

3.3. Fragmentation pattern of standard GN A

To efficiently identify metabolites in the biological sample, the retention time (RT) in the UPLS chromatogram, MS spectrum and MS^2 fragmentation patterns were confirmed using reference GN A (Fig. 3A). The parent ion was deprotonized at m/z 352.0067 ($[M\text{-}H]^-$) in the negative ionization mode. Using MassFragment™, the major MS/MS spectra produced were determined at m/z 161.0353 ($C_8H_5N_2O_2$), 189.0316 ($C_9H_5N_2O_3$), 218.0556 ($C_{10}H_8N_3O_3$), 220.9996 ($C_9H_5N_2O_3S$), 239.0456 ($C_{13}H_7N_2O_3$), 253.0487 ($C_{10}H_{11}N_3O_3S$), 257.0438

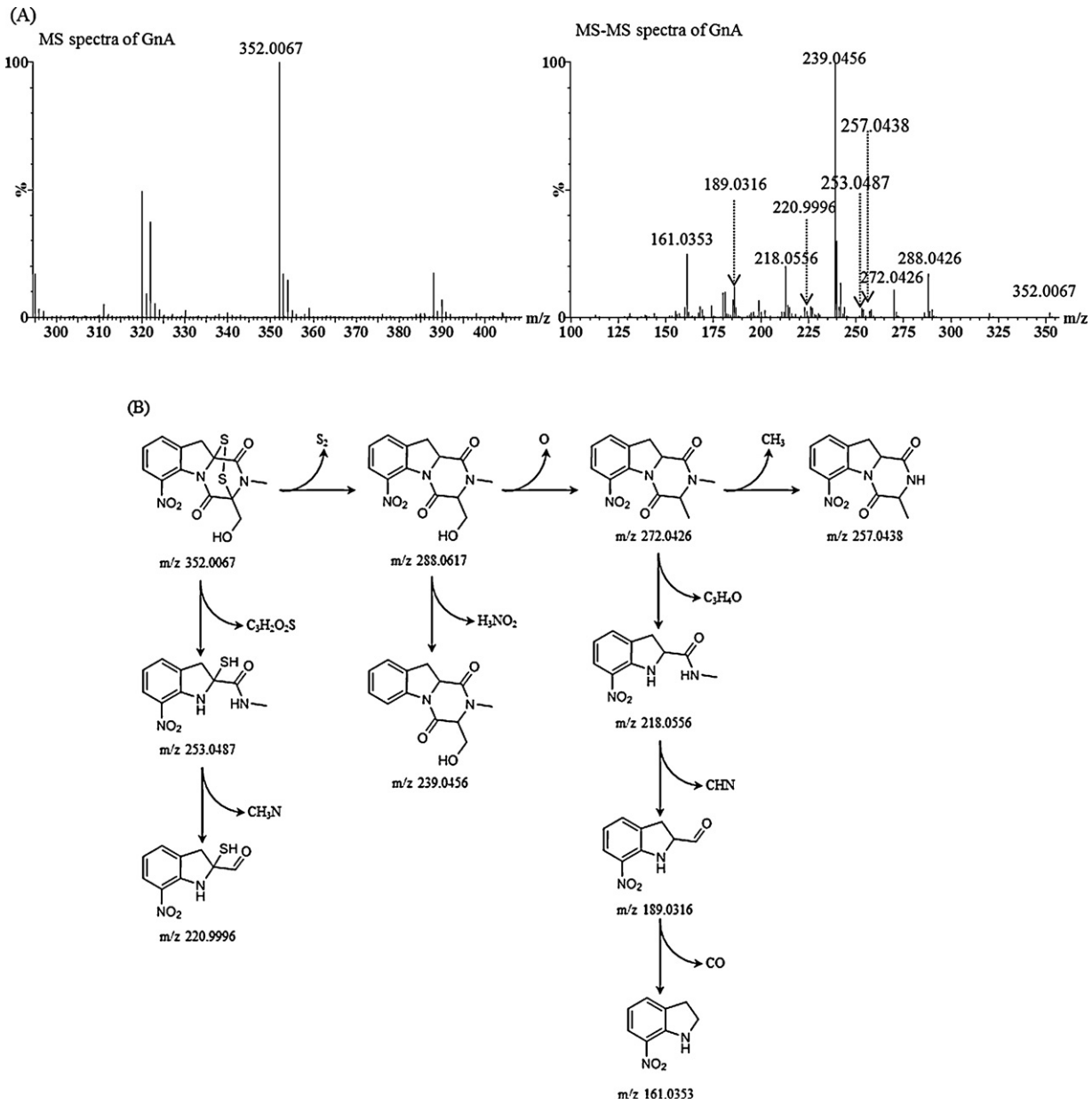

Fig. 3. MS and MS–MS analysis of reference GN A: (A) MS and MS–MS spectra of GN A and (B) predicted fragmentation patterns of GN A.

($C_{12}H_7N_3O_4$), 272.0426 ($C_{13}H_{10}N_3O_4$) and 288.0617 ($C_{13}H_{10}N_3O_5$) (Table 1). These spectra were considered to be formed by the sequential loss of a S_2, O, or CH_3 as well as ring cleavage. The predicted fragmentation pattern of GN A is shown in Fig. 3B. The MS/MS fragmentation pattern of the parent molecule was useful in understanding the structures of the metabolites.

3.4. Identification of metabolites

Reduction, nitro-reduction and hydration were the primary metabolic processes affecting GN A *in vivo*, followed by demethylation or oxidative deamination to alcohol, as well as cysteine, glycine, glucuronide or sulfate conjugation (Fig. 4). Table 2 shows

Table 1
The possible elemental compositions, measured and calculated masses, mass errors of deprotonated GN A and its fragment ions and loss of groups in fragmentation.

Elemental composition	Measured mass (Da)	Calculated mass (Da)	Error (mDa)	Loss
$C_{13}H_{10}N_3O_5S_2$	352.0067	352.0062	+0.5	
$C_8H_5N_2O_2$	161.0353	161.0351	+0.2	$C_5H_5NO_3S_2$
$C_9H_5N_2O_3$	189.0316	189.0300	+1.6	$C_4H_5NO_2S_2$
$C_{10}H_8N_3O_3$	218.0556	218.0566	−1.0	$C_3H_4O_2S_2$
$C_9H_5N_2O_3S$	220.9996	221.0021	−2.5	$C_4H_5NO_2S$
$C_{13}H_7N_2O_3$	239.0456	239.0457	−0.1	$H_3NO_2S_2$
$C_{10}H_{11}N_3O_3S$	253.0487	253.0521	−3.4	$C_3H_2O_2S$
$C_{12}H_7N_3O_4$	257.0438	257.0437	+0.1	CH_3OS_2
$C_{13}H_{10}N_3O_4$	272.0426	272.0671	−24.5	OS_2
$C_{13}H_{10}N_3O_5$	288.0617	288.0620	−0.3	S_2

Table 2
The RT, parent ions, fragment ions, their formula presented by elemental composition, mass error between the calculated and measured ions and loss of groups in fragmentation.

Compound no.	RT (min)	Molecular ion *m/z* (Da)	Fragment ion *m/z* (Da)	Formula	Error (mDa)	Loss	Relative peak ratio[a]
G0	8.25	352.0095		$C_{13}H_{10}N_3O_5S_2$	+3.3		1
			189.0321	$C_9H_5N_2O_3$	+9.9	$C_4H_5NO_2S_2$	
			218.0616	$C_{10}H_8N_3O_3$	+5.0	$C_3H_4O_2S_2$	
			253.0491	$C_{10}H_{11}N_3O_3S$	−3.0	$C_3H_2O_2S$	
			257.0369	$C_{12}H_7N_3O_4$	−6.8	CH_3OS_2	
			288.0639	$C_{13}H_{10}N_3O_5$	+1.9	S_2	
G1	5.99	322.029		$C_{13}H_{13}N_3O_3S_2$	12.7		6.06
			160.0399	$C_9H_8N_2O$	−10.2	$C_4H_5NO_2S_2$	
			188.0711	$C_{10}H_{10}N_3O$	−11.3	$C_3H_3O_2S_2$	
			227.0867	$C_{12}H_9N_3O_2$	−10.7	CH_4OS_2	
			240.0421	$C_{12}H_6N_3O_3$	+1.2	CH_7S_2	
			258.0861	$C_{13}H_{12}N_3O_3$	−1.8	HS_2	
G2	3.05	308.0092		$C_{12}H_{12}N_3O_3S_2$	−7.2		2.02
			160.0399	$C_9H_8N_2O$	−23.8	$C_3H_4NO_2S_2$	
			227.0828	$C_{12}H_9N_3O_2$	+13.3	CH_3OS_2	
			244.0928	$C_{12}H_{10}N_3O_3$	+12.8	H_2S_2	
G3	6.45	441.0558		$C_{16}H_{17}N_4O_7\ S_2$	+1.9		2.71
			121.0284	$C_3H_7NO_2S$	+8.6	$C_{13}H_{10}N_3O_5S$	
			230.0208	$C_{11}H_8N_3OS$	−13.6	$C_5H_9NO_6S$	
			253.0512	$C_{10}H_{11}N_3O_3S$	−0.9	$C_6H_6NO_4S$	
			321.0429	$C_{13}H_{11}N_3O_5S$	+1.0	$C_3H_6NO_2S$	
G4	5.20	354.0297		$C_{13}H_{12}N_3O_5S_2$	9.2		9.15
			218.0703	$C_{10}H_3N_3O_3$	+13.7	$C_3H_4O_2S_2$	
			253.0499	$C_{10}H_{11}N_3O_3S$	−2.2	C_3HO_2S	
			257.0825	$C_{13}H_{11}N_3O_3$	+2.5	HO_2S_2	
			273.0759	$C_{13}H_{11}N_3O_4$	+0.9	HOS_2	
			288.0870	$C_{13}H_{10}N_3O_5$	+25.0	H_2S_2	
G5	3.50	340.0233		$C_{12}H_{11}N_3O_5S_2$	+17.1		13.41
			204.0291	$C_{10}H_6NO_2S$	+17.2	$C_2H_5N_2O_3S$	
			253.0470	$C_{10}H_{11}N_3O_3S$	−5.1	C_2O_2S	
			258.0436	$C_{12}H_8N_3O_4$	−7.9	H_2OS_2	
			274.0550	$C_{12}H_8N_3O_5$	−7.0	H_3S	
G6	4.37	530.0576		$C_{19}H_{20}N_3O_{11}S_2$	3.7		2.94
			188.9862	$C_9H_5N_2O_3$	−43.8	$C_{10}H_{15}NO_8S_2$	
			218.1030	$C_{10}H_8N_3O_3$	+46.4	$C_9H_{12}O_8S_2$	
			253.0464	$C_{10}H_{11}N_3O_3S$	−5.7	$C_{10}H_9O_8S$	
			257.0780	$C_{13}H_{11}N_3O_3$	−2.0	$C_2H_5N_2O_3S$	
G7	6.20	324.0473		$C_{13}H_{15}N_3O_3S_2$	−0.4		4.18
			160.0327	$C_9H_8N_2O$	−31.0	$C_4H_7NO_2S_2$	
			242.0903	$C_{13}H_{12}N_3O_2$	−2.7	H_3OS_2	
			244.0729	$C_{12}H_{10}N_3O_3$	+0.7	CH_5OS_2	
			258.0517	$C_{13}H_{12}N_3O_3$	−36.2	H_3S_2	
G8	5.40	325.0381		$C_{13}H_{13}N_2O_4S_2$	6.4		27.04
			116.0171	C_4H_6NOS	+0.1	$C_9H_7NO_3S$	
			161.0387	$C_9H_7NO_2$	−9.0	$C_4H_6NO_2S_2$	
			220.0378	$C_{10}H_8N_2O_2S$	+7.1	$C_3H_5O_2S$	
			243.0761	$C_{13}H_{11}N_2O_3$	−0.9	$H_2O_3S_2$	
			276.0905	$C_{13}H_{12}N_2O_3S$	+33.6	HOS	
G9	7.55	404.0043		$C_{13}H_{12}N_2O_7S_3$	−5.6		80.20
			116.0486	C_4H_6NOS	+8.5	$C_9H_6NO_6S_2$	
			161.0353	$C_9H_7NO_2$	−0.9	$C_4H_5NO_5S_3$	
			242.0125	$C_{12}H_8N_2O_2S$	−2.7	$CH_4O_5S_2$	
			276.0701	$C_{13}H_{12}N_2O_3S$	−13.1	O_4S_2	
G10	6.55	370.0291		$C_{13}H_{12}N_3O_6S_2$	12.3		2.27
			113.0244	$C_4H_3NO_3$	+13.1	$C_9H_9N_2O_3S_2$	
			244.0738	$C_{12}H_{10}N_3O_3$	+1.6	$CH_2O_3S_2$	
			268.0382	$C_{13}H_6N_3O_4$	+2.4	$H_6O_2S_2$	
			273.0767	$C_{13}H_{11}N_3O_4$	+1.7	HO_2S_2	
G11	6.20	340.0504		$C_{13}H_{14}N_3O_4S_2$	+1.2		4.18
			113.0246	$C_4H_3NO_3$	+13.3	$C_9H_{11}N_2OS_2$	
			216.0782	$C_{11}H_{10}N_3O_2$	+0.9	$C_2H_4O_2S_2$	
			244.0728	$C_{12}H_{10}N_3O_3$	+0.6	CH_2NOS_2	
			257.0824	$C_{13}H_{11}N_3O_3$	+2.4	H_3OS_2	
G12	2.40	427.0444		$C_{15}H_{15}N_4O_7S_2$	+6.2		0.83
			113.0247	$C_4H_3NO_3$	+13.4	$C_{11}H_{12}N_3O_4S_2$	
			244.0487	$C_{12}H_{10}N_3O_3$	−15.7	$C_{13}H_{13}N_2O_4S_2$	
			268.0514	$C_{13}H_6N_3O_4$	+15.6	$C_2H_9NO_3S_2$	

Table 2 (*Continued*)

Compound no.	RT (min)	Molecular ion *m*/*z* (Da)	Fragment ion *m*/*z* (Da)	Formula	Error (mDa)	Loss	Relative peak ratio[a]
			328.0456	$C_{14}H_8N_4O_6$	+1.2	CH_7OS_2	
G13	4.50	338.0037		$C_{12}H_9N_3O_5S_2$	13.4		2.89
			175.0249	$C_9H_7N_2O_2$	−25.8	$C_3HNO_3S_2$	
			189.0039	$C_9H_5N_2O_3$	−26.1	$C_3H_3NO_2S_2$	
			221.0846	$C_{10}H_9N_2O_4$	+28.5	C_2NOS_2	
			253.0423	$C_{10}H_9N_2O_4S$	+14.0	C_2NOS	

[a] Relative peak ratio were calculated on the basis of BPI chromatogram as follows: (relative peak ratio) = (the peak area of metabolite)/(the peak area of parent, G0).

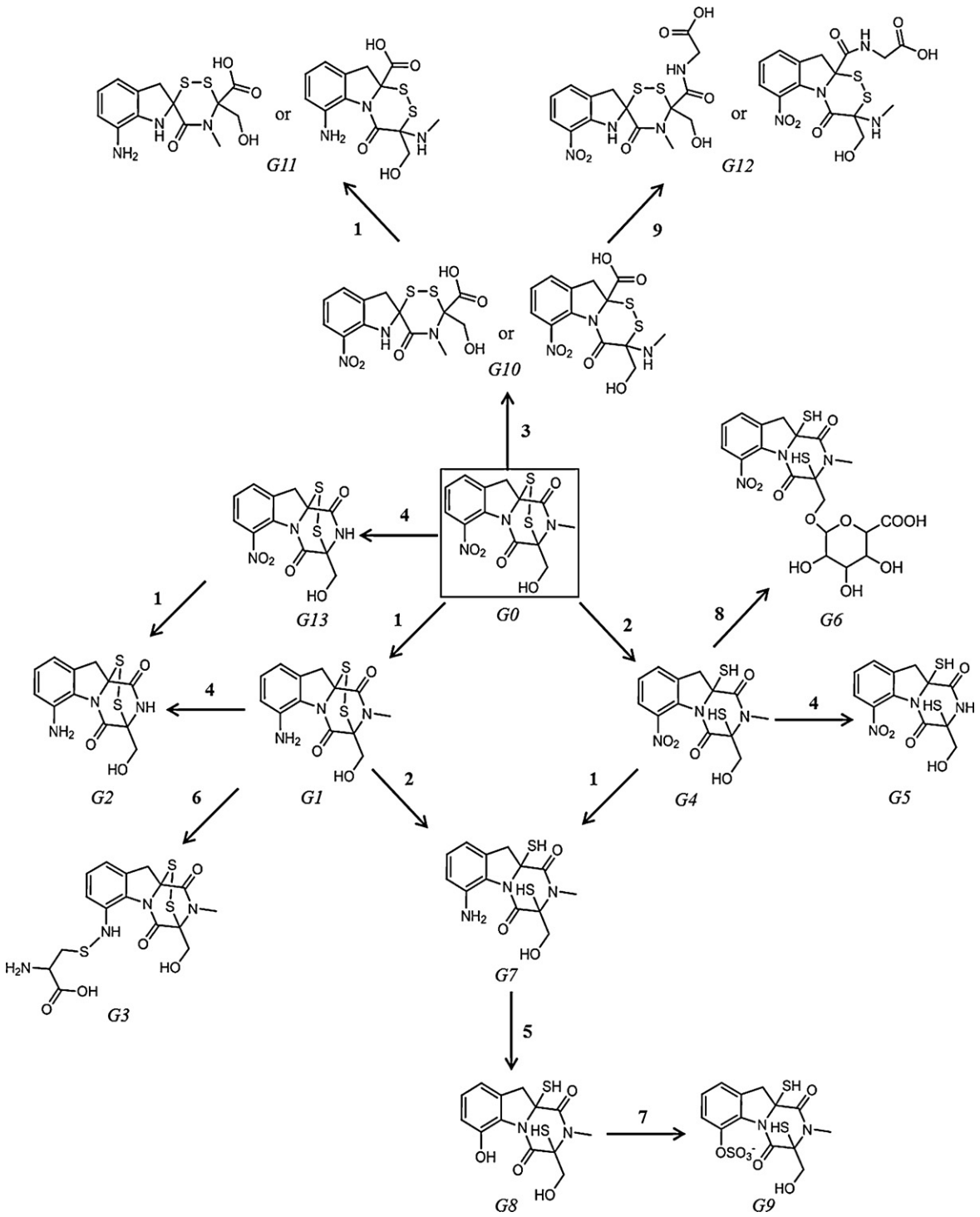

Fig. 4. Predicted metabolic pathways of GN A in rat urine. (1) Nitro-reduction; (2) reduction; (3) hydrolysis; (4) demethylation; (5) oxidative deamination to alcohol; (6) cysteine conjugation; (7) sulfate conjugation; (8) glucuronide conjugation; (9) glycine conjugation.

the RT, parent ions, fragment ions, their formula by elemental compositions, the mass error between the calculated and measured ions and the loss of groups in the fragmentation for each metabolite as well as relative peak ration which could be useful to estimate the main metabolites.

3.4.1. Parent compound (G0)

The non-metabolized GN A was detected at a RT of 8.25 min with $[M-H]^-$ ions at *m/z* 352.0095 in rat urine. The MS^2 fragment ions were investigated at *m/z* 189.0321 ($C_9H_5N_2O_3$), 218.0616 ($C_{10}H_8N_3O_3$), 253.0491 ($C_{12}H_7N_3O_4$), 257.0369 ($C_{12}H_7N_3O_4$) and 288.0639 ($C_{13}H_{10}N_3O_5$), the same as those of standard GN A.

3.4.2. Metabolites from nitro reduced GN A (G1–G3)

G1 was eluted at an RT of 5.99 min with the $[M-H]^-$ ions at *m/z* 322.029 ($C_{13}H_{13}N_3O_3S_2$) and showed a 30 Da mass difference compared to GN A (GN A-O_2 + H_2). Its fragment ions were investigated at *m/z* 160.0399 ($C_9H_8N_2O$), 188.0711 ($C_{10}H_{10}N_3O$), 227.0867 ($C_{12}H_9N_3O_2$), 240.0421 ($C_{12}H_6N_3O_3$) and 258.0861 ($C_{13}H_{12}N_3O_3$). The ions at *m/z* 188.0711, 227.0867 and 258.0861 also displayed a 30 Da mass shift from the MS/MS ions as compared with the elemental compositions of GN A, which were 218.0616 ($C_{10}H_8N_3O_3$), 257.0369 ($C_{12}H_7N_3O_4$) and 288.0639 ($C_{13}H_{10}N_3O_5$), respectively. From the mass spectrum patterns, G1 is believed to be a nitro-reduced metabolite of GN A. Generally, nitroaromatic compounds are converted to the corresponding amines by nitroreductase, which is called nitro-reduction ($NO_2 \rightarrow NH_2$) [5]. The toxic effects of nitro-aromatic compounds and aromatic amines have been well-established [6]. Reduction of nitrogroups on nitroaromatic compounds and oxidation of amine groups on aromatic amines generate the same kind of electrophilic reactive intermediates (N-hydroxylamines) although these reactions occur at different locations [6]. Some corresponding pairs of nitro-aromatic compounds and aromatic amines show the toxicities at the same time. For instance, 1-nitropyrene (1-NP) is metabolized to 1-aminopyrene (1-AP) via nitro-reduction *in vivo* [7,8]. Both of them showed the toxicities although they could behave in very different ways against the organism [9]. Thus, G1, aromatic amine derived from GN A by nitroreduction might be a toxic metabolite. However this speculation remains to be explored.

G2 was detected in the chromatographic peak at 3.05 min with the $[M-H]^-$ ion at *m/z* 308.0092 ($C_{12}H_{12}N_3O_3S_2$), which was 14 Da lower than that of G1 (G1-CH_2). Its MS/MS fragmentation analysis suggested ions at *m/z* 160.0399 ($C_9H_8N_2O$) and 227.0867 ($C_{12}H_9N_3O_2$), the same as those of G1, as well as 244.0928 ($C_{12}H_{10}N_3O_3$), with a 14 Da mass difference from the ion at *m/z* 288.0632 of G1. Accordingly, G2 is believed to be a demethylated derivative of G1.

G3 was found to be another metabolite related to G1. It was found at an RT of 6.45 min with the deprotonated molecular ion at *m/z* 441.0558 ($C_{16}H_{17}N_4O_7S_2$). Its MS/MS spectrum showed notable product ions at *m/z* 321.0429 ($C_{13}H_{11}N_3O_5S$; loss of cysteine conjugate) and 121.0284 ($C_3H_7NO_2S$; cysteine conjugate), which were generated from the cleavage of the S—C bond by high collision energy. As the SH group of cysteine could easily be attached to the amine group linked to aromatic compounds with a π-bond [10], G3 was determined to be a cysteine S-conjugate to the aromatic amine of G1.

3.4.3. Metabolites from reduced GN A (G4–G6)

G4 was found on the chromatogram with an RT of 5.2 min and MS spectrum at *m/z* 354.0332 ($C_{13}H_{12}N_3O_5S_2$), which was 2 Da higher than the deprotonated ion of GN A (GN A + H_2), indicating that G4 is a reduced metabolite. Its MS/MS fragmentation pattern presented the main product ions at *m/z* 218.0612 ($C_{10}H_8N_3O_3$), 253.0487 ($C_{10}H_{11}N_3O_3S$) and 288.0632 ($C_{13}H_{10}N_3O_5$), which were the same as that produced by the fragmentation of GN A. Additionally, ions at *m/z* 257.0825 ($C_{13}H_{11}N_3O_3$) and 273.0759 ($C_{13}H_{11}N_3O_4$) were detected, which were produced via loss of the HO_2S_2 and HOS_2 groups, respectively. GN A has a unique transannular disulfide bridge, which is essential for biological effects of epipolythiodioxopiperazines (ETPs) [11]. A lot of studies have reported that ETPs are secondary metabolites of fungi with bioactivities including antinematodal, anticancer, antimicrobial, and cytotoxicity [12–15]. Gliotoxin is the prototype of EPTs and has been extensively studied in various ways [16]. Comprehensive molecular studies have reported that the disulfide bridge of gliotoxin is indispensable for its biological activities via at least two ways: formation of reactive oxygen species (ROS) through redox cycling between the reduced (dithiol) and oxidized (disulphide) forms [17] and/or conjugation with susceptible thiol residues of target proteins [18]. The previous study demonstrated that gliotoxin is mainly reduced to the dithiol form in animal cells implying that the reduced metabolite play critical roles in its biological activity via redox cycling [19]. Additionally, the toxicity of sporidesmin, another EPT, was reported to be modulated by ROS [20], suggesting that redox cycling is significant mechanism of hazardous effects. Just as gliotoxin and other EPTs, GN A can be reduced to generate a dithiol form which might be important for its bioactivities. Thus, G4 is believed to be a reduced metabolite with a dithiol, an active functional group.

G5 was found at an RT of 3.50 min as a deprotonized ion with *m/z* 340.0233 ($C_{12}H_{11}N_3O_5S_2$), with a14 Da mass shift from G4 (G4-CH_2), suggesting that G5 was generated through the demethylation of G4. Its product ions were obtained at *m/z* 204.0291 ($C_{10}H_6NO_2S$), 253.0470 ($C_{10}H_{11}N_3O_3S$), 258.0436 ($C_{12}H_8N_3O_4$) and 274.0395 ($C_{12}H_8N_3O_5$). The ion at *m/z* 258.0436 was produced by loss of S_2 and H_2O, and the ion at *m/z* 253.0470 was the same as that of G4. The ions at *m/z* 204.0291 and 274.0395 were at a 14 Da mass shift from those at *m/z* 218. 0612 and 288.0632 of G4, respectively, confirming that G5 resulted from the demethylation of G4.

The chromatogram of G6 was detected at an RT of 4.37 min with an $[M-H]^-$ ion at *m/z* 530.0576 ($C_{19}H_{20}N_3O_{11}S_2$), 176 Da ($C_6H_8O_6$) higher than that of G4. The notable product ions were detected at *m/z* 113.0238 ($C_5H_5O_3$) and 175.0253 ($C_6H_7O_6$) as well as 253.0464 ($C_{10}H_{11}N_3O_3S$) and 257.0780 ($C_{13}H_{11}N_3O_3$), which were the same as those of G4. When O-glucuronide conjugates of parent compounds are analyzed with electrospray ionization (ESI) mass spectrometry, MS/MS spectra presented characteristic fragment ions at *m/z* 113 and 175 in the negative ionization mode, derived from the glucuronide moiety of the parent molecules [21]. Therefore, we propose that G6 is an O-glucuronide conjugate of G4.

3.4.4. Metabolites G7–G9

The deprotonated ions of G7and G8 were recognized at *m/z* 324.0473 ($C_{13}H_{15}N_3O_3S_2$) and 325.0381 ($C_{13}H_{13}N_2O_4S_2$) in the chromatographic peaks with an RT of 6.20 and 5.4 min, respectively. A mass difference of 30 Da between the parent ions, G4 and G7 was observed, and the ion of G7 at *m/z* 258.0517 ($C_{13}H_{12}N_3O_3$) also presented a 30 Da mass shift from the ion of G4 at *m/z* 288.0632, which suggested that the —NO_2 group of G4 was biotransformed into an —NH_2 group through nitro reduction, resulting in G7. Additionally, G7could be created via the reduction of the sulfide bond in G1, based on a comparison of the suggested mass values and elemental compositions of G1 and G7 (2 Da shift; H_2). G7 was further converted to G8. The mass difference between G7 and G8 was 0.99, and some of their product ions presented similar patterns; ions were found at *m/z* 160.0327 (G7; $C_9H_8N_2O$) *versus* 161.0387 (G8; $C_9H_7NO_2$) as well as at 242.0903 (G7; $C_{13}H_{12}N_3O_2$) *versus* 243.0761 (G8; $C_{13}H_{11}N_2O_3$). Primary amines linked to aromatic rings are easily oxidized to deamination products [22,23]. Therefore, the NH_2

group in G7 was transformed to an OH group by oxidative deamination to alcohol, deriving the metabolite G8.

G9 was found at an RT of 7.55 min with the $[M-H]^-$ ion at m/z 404.0043 ($C_{13}H_{12}N_2O_7S_3$). The fragment ions were recognized at m/z 116.0486 (C_4H_6NOS), 161.0353 ($C_9H_7NO_2$), 242.0125 ($C_{12}H_8N_2O_2S$) and 276.0701 ($C_{13}H_{12}N_2O_3S$), which were similar to those of G8. The mass difference between G8 and G9 was 80 Da (SO_3), and G8 had a hydroxyl group attached to an aromatic ring. We believe that G9 is a sulfate conjugate of G8. According to relative peak ratio of metabolites, G7–G9 might be major metabolites, especially, sulfate conjugate form G9 (Table 2). As analytical methods in present study were not optimized for quantification of each metabolite, further studies are needed to confirm the main metabolites and dominant metabolism pathways.

3.4.5. Metabolites related to hydrolyzed GN A (G10–G12)

Metabolites G10–G12 were eluted at RTs of 6.55, 6.20 and 2.40 min with the $[M-H]^-$ ions at m/z 370.0291 ($C_{13}H_{12}N_3O_6S_2$), 341.0504 ($C_{13}H_{14}N_3O_4S_2$) and 427.0444 ($C_{15}H_{15}N_4O_7S_2$), respectively. The products in their MS/MS fragmentation analysis at m/z 113.0244 ($C_4H_3NO_3$), 244.0738 ($C_{12}H_{10}N_3O_3$) and 268.0382 ($C_{13}H_6N_3O_4$) were commonly detected. Their fragmentation patterns were similar compared to each other, but distinct from other metabolites. The elemental composition analysis suggested that the parent ion of G10 had additional H_2O in comparison with GN A, indicating that G10 is a hydrolyzed molecule of GN A. GN A contains two amide linkages in its structure, which are easily cleaved by hydrolysis. G10 can be in two different forms, but both had the same fragmentation pattern based on MassFragment analysis. A further search for a product ion suggested that G11 is a metabolite transformed through the nitro reduction of G10, given that G11 is 30 Da lighter than G10. G12 displayed the elemental composition [$C_{13}H_{12}N_3O_6S_2 + C_2H_5NO_2$ (glycine moiety)$-H_2O$], and the 57 Da mass shift from G10 indicates that G12 is a glycine conjugate of G10.

3.4.6. Metabolites related to demethylated GN A (G13)

G13 was observed at an RT of 4.50 min with the molecular ion at m/z 338.0037 ($C_{12}H_9N_3O_5S_2$). The fragment ions were found at m/z 175.0249 ($C_9H_7N_2O_2$), 189.0039 ($C_9H_5N_2O_3$), 221.0846 ($C_{10}H_9N_2O_4$) and 253.0418 ($C_{10}H_9N_2O_4S$). Its parent ion at m/z 338.0037 and its product ion at 175.0249 showed a 14 Da MS difference when compared to the deprotonated ion of GN A and its fragment ion at m/z 189.0321 ($C_9H_5N_2O_3$), implying that G13 is an N-demethylation metabolite of GN A. Some drugs with the N-CH3 group at a similar position in their structures are converted to N-demethylated metabolites by cytochrome p-450 enzymes [24,25]. Thus, GN A can lose its methyl group by CYP enzyme activity, resulting in G13.

4. Conclusions

In present study, the potential metabolites of GN A, a new drug candidate, were identified using UPLC–QTOP-MS analysis followed by the elucidation of the metabolite structure with the assistance of MetaboLynx™ and MassFragment™. After a single intravenous administration of GN A, the parent molecule and its metabolites were detected in rat urine containing a complicated matrix of compounds. The predicted metabolites were derived via reduction, nitro-reduction, hydrolysis, demethylation and deamination to alcohol, as well as glycine, cysteine, sulfate and glucuronide conjugation. The reduced GN A was found to be a molecule with a dithiol group, which was then further demethylated, reduced at the aromatic nitro group or conjugated with glucuronide. The nitro reduced metabolite is believed to be an aromatic amine corresponding to GN A, which was biotransformed through demethylation, reduction and conjugation with cysteine. The metabolite with the dithiol and aromatic amine group was further metabolized by deamination to alcohol, followed by sulfur conjugation. The molecule resulting from hydrolysis was converted into a nitro-reduced metabolite or glycine conjugate. Reduced GN A and the nitro-reduced metabolite may present pharmacological or toxicological activities, which is valuable information in terms of further drug development for GN A. In addition, this work has shown that the UPLC–QTOP-MS analysis coupled with an efficient data processing program is useful for the rapid and reliable characterization of GN A metabolites *in vivo*.

Appendix A. Supplementary data

Supplementary data associated with this article can be found, in the online version, at http://dx.doi.org/10.1016/j.jchromb.2012.08.015.

References

[1] H.B. Park, H.C. Kwon, C.H. Lee, H.O. Yang, J. Nat. Prod. 72 (2009) 248.
[2] Y. Liang, G. Wang, L. Xie, L. Sheng, Curr. Drug Metab. 12 (2011) 329.
[3] M. Zhu, H. Zhang, W.G. Humphreys, J. Biol. Chem. 286 (2011) 25419.
[4] K. Yu, D. Little, R. Plumb, B. Smith, Rapid Commun. Mass Spectrom. 20 (2006) 544.
[5] I.T. Reeve, M.G. Miller, Chem. Res. Toxicol. 15 (2002) 352.
[6] H.G. Neumann, C. van Dorp, I. Zwirner-Baier, Toxicol. Lett. 82–83 (1995) 771.
[7] K. El-Bayoumy, C. Sharma, Y.M. Louis, B. Reddy, S.S. Hecht, Cancer Lett. 19 (1983) 311.
[8] T. Kinouchi, Y. Manabe, K. Wakisaka, Y. Ohnishi, Microbiol. Immunol. 26 (1982) 993.
[9] M.J. Edwards, J.M. Parry, S. Batmanghelich, K. Smith, Mutat. Res. 163 (1986) 81.
[10] G. Sabbioni, C.R. Jones, Biomarkers 7 (2002) 347.
[11] D.M. Gardiner, P. Waring, B.J. Howlett, Microbiology 151 (2005) 1021.
[12] H. Minato, M. Matsumoto, T. Katayama, J. Chem. Soc. Perkin Trans. 1 (17) (1973) 1819.
[13] M. Chu, I. Truumees, M. Patel, C. Blood, P.R. Das, M.S. Puar, J. Antibiot. 48 (1995) 329.
[14] J.Y. Dong, H.P. He, Y.M. Shen, K.Q. Zhang, J. Nat. Prod. 68 (2005) 1510.
[15] O. Sterner, E. Thines, F. Eilbert, H. Anke, J. Antibiot. 51 (1998) 228.
[16] D.H. Scharf, N. Remme, T. Heinekamp, P. Hortschansky, A.A. Brakhage, C. Hertweck, J. Am. Chem. Soc. 132 (2010) 10136.
[17] C.R. Isham, J.D. Tibodeau, W. Jin, R. Xu, M.M. Timm, K.C. Bible, Blood 109 (2007) 2579.
[18] K.J. Kwon-Chung, J.A. Sugui, Med. Mycol. 47 (Suppl. 1) (2009) S97.
[19] P.H. Bernardo, N. Brasch, C.L. Chai, P. Waring, J. Biol. Chem. 278 (2003) 46549.
[20] R. Munday, Chem. Biol. Interact. 41 (1982) 361.
[21] D.F. Zhong, X.Y. Chen, J.K. Gu, Fresen. J. Anal. Chem. 365 (1999) 553–558.
[22] H. Kurebayashi, A. Tanaka, T. Yamaha, A. Tatahashi, Xenobiotica 18 (1988) 1039.
[23] M.R. Parsons, M.A. Convery, C.M. Wilmot, K.D. Yadav, V. Blakeley, A.S. Corner, S.E. Phillips, M.J. McPherson, P.F. Knowles, Structure 3 (1995) 1171.
[24] U.A. Boelsterli, A. Lanzotti, C. Goldlin, M. Oertle, Drug Metab. Dispos. 20 (1992) 96.
[25] B. Kleingeist, R. Bocker, G. Geisslinger, R. Brugger, J. Pharm. Pharm. Sci. 1 (1998) 38.